

Calculation of overdamped c-axis charge dynamics and the coupling to polar phonons in cuprate superconductors.

W. Meevasana,^{1,*} T.P. Devereaux,² N. Nagaosa,³ Z.-X. Shen,¹ and J. Zaanen^{1,†}

¹*Department of Physics, Applied Physics, and Stanford Synchrotron Radiation Laboratory, Stanford University, Stanford, CA 94305*

²*Department of Physics, University of Waterloo, Waterloo, Ontario, Canada N2L 3G1*

³*CREST, Department of Applied Physics, University of Tokyo, Bunkyo-ku, Tokyo 113, Japan*

(Dated: October 4, 2006)

In our recent paper we presented empirical evidences suggesting that electrons in cuprate superconductors are strongly coupled to unscreened c-axis polar phonons. In the overdoped regime the c-axis metallizes and we present here simple theoretical arguments demonstrating that the observed effect of the metallic c-axis screening on the polar electron-phonon coupling is consistent with a strongly overdamped c-axis charge dynamics in the optimally doped system, becoming less dissipative in the overdoped regime.

PACS numbers: 71.38.-k, 74.72.Hs, 79.60.-i

I. INTRODUCTION

As electrodynamic media the cuprate high- T_c superconductors are highly anomalous. In their normal state they behave like metals in the planar ab-directions while they can be regarded as dielectrics along the interplanar c-direction, at least at finite frequencies. Only in the regime where the superconductivity start to degrade because of too high doping levels, metallic ‘normalcy’ develops along the c-axis¹.

Electrodynamical ‘anomaly’ raises a general question regarding the nature of electron-phonon coupling in the cuprates. Insulating cuprates are as any other oxide characterized by a highly polarizable lattice. The consequence is that one is dealing with strongly ‘polar’ electron-phonon (EP) couplings, associated with the long range nature of the Coulomb interaction between carriers and the ionic lattice². In normal metals these long range interactions are diminished by metallic screening and one is left with rather weak, residual short range EP interactions. Although this is also the case in the planar directions of the cuprates, due to incoherent electron motion perpendicular to the planes we argue that the c-axis phonons are largely unscreened in this direction and strong polar EP-couplings are active³.

In our recent paper⁴, angle-resolved photoemission (ARPES) studies of optimally-doped and overdoped $\text{Bi}_2\text{Sr}_2\text{CuO}_6$ (Bi2201) superconductors have indicated that polar c-axis couplings play an important role. Energy dispersion “kinks” resulting from coupling to well defined bosonic modes, which we argued to be phonons rather than spin resonance modes, are weaker at low binding energies in overdoped compared to optimally doped Bi2201. This case is twofold: (a) a good description is obtained for the electronic self-energy in the nodal momentum direction in an optimally doped single layer Bi2201 superconductor by assuming that the Eliashberg function $\alpha^2F(\omega)$ largely coincides with the measured c-axis electron energy loss function; (b) The electronic self-

energy drastically changes in a strongly overdoped system and we show that these changes are accounted for assuming a frequency dependent screening characterized by a scale $\omega_{scr,c} \simeq 60\text{meV}$. Here we will present calculations further substantiating this claim. We will give the reasons why the c-axis optical loss function should be a good model for the Eliashberg function associated with the polar couplings in the optimally doped system. Furthermore, we will show that the way the self-energy diminishes in the overdoped regime is qualitatively- and quantitatively consistent with what has been learned from optical measurements about the way metallicity develops in the overdoped regime.

We remark that a great deal of focus has been placed on in-plane phonons such as the breathing modes showing large softenings with doping in the cuprates⁵. These modes have been shown to contribute to the electronic self-energy for nodal electrons⁶. Moreover, the breathing phonons provide signatures on the spectral function for the formation of charge ordering⁷ and may contribute to d -wave pairing in the presence of strong correlations⁸. Rather than taking into account the interesting and relevant issue of planar phonon couplings, our focus here will be on the c -axis phonons in order to explore the role of screening.

The c-axis is insulating, not because a lack of carriers, but instead due to the fact that charge dynamics is strongly overdamped and incoherent. To be discussed at the end, the damping rate is decreasing rapidly in the overdoped regime, and this is exactly what is needed to explain the behavior of the self-energy. Van der Marel and Kim⁹ pointed out some time ago that the *effective* c-axis plasmon frequency $\omega_{p,c} = 4\pi n_c e^2 / m_c$ (n_c and m_c are the c-axis effective carrier density and band mass, respectively) as determined by an optical sum rule can be as large as 1/4 of the planar plasma frequency $\omega_{p,ab} \simeq 1\text{eV}$ ¹⁰. The essence of overdamped dynamics is captured by the expression for the dielectric function associated with a plasmon with damping rate Γ and frequency $\omega_{p,c}$

at long wavelengths,

$$\epsilon_{el}(\omega) = \epsilon_{\infty} - \frac{\omega_{p,c}^2}{(\omega^2 + i\omega\Gamma)} \quad (1)$$

It is demonstrated (see Eq. (17) that in the overdamped case $\Gamma \gg \omega_{p,c}$ the medium behaves like a dielectric at frequencies larger than the characteristic frequency,

$$\omega_{scr,c} \approx \frac{\omega_{p,c}}{\epsilon_{\infty}\Gamma} \omega_{p,c} \quad (2)$$

In the cuprates, it will be shown that in the doping range up to optimal doping, this frequency is smaller than the typical optical phonon frequencies with the effect that the c-axis optical conductivity $\sigma_c^1(\omega)$ looks like that of a polar insulator, dominated by unscreened polar phonons. To get the impression of the magnitude of $\omega_{scr,c}$, we assume a simple Drude form for the optical conductivity (see Eq. (18)). With this form, $\omega_{scr,c}$ is approximately proportional to the height of the electronic background in the c-axis $\sigma_c^1(\omega)$ and this background is found to increase rapidly in the overdoped regime in LSCO system¹¹. We find that this change is just of the right magnitude to explain the changes in the self-energy of the overdoped system.

The justification for taking the *c-axis* EP couplings being representative of the interactions showing up in the self-energy will be discussed first. The actual importance of polar EP-couplings in the cuprates is *a priori* a rather subtle affair. On the one hand, there are actually very few phonons which can be regarded as unscreened. The cuprates can be viewed as a stack of metallic sheets. For one limit, when considering phonons with \vec{q} purely along c-axis ($\vec{q} = \vec{q}_c$), the screening frequency $\omega_{scr,c}$ should be set by the effective c-axis plasmon frequency $\omega_{p,c}$, such that all phonons with frequency $\omega_{ph,i}(\vec{q} = \vec{q}_c) < \omega_{scr,c}$ can be regarded as screened. This $\omega_{scr,c}$ will be later shown to be defined by Eq. (17). Similarly, for the other limit, when considering phonons with \vec{q} purely in the ab-plane ($\vec{q} = \vec{q}_{ab}$), $\omega_{scr,ab}$ should be set by the planar plasmon frequency $\omega_{p,ab}$. Since $\omega_{p,ab}$ is large compared to $\omega_{p,c}$ ¹⁰, this implies that phonons with \vec{q} along the c-axis will be left unscreened compared to phonons with \vec{q} in ab plane. In a more general case, at a 3D momentum $\vec{q} = \vec{q}_{ab} + \vec{q}_c$, the effective 3D plasmon frequency $\omega_{p,\vec{q}}$ for $\vec{q} \rightarrow 0$ ^{9,12} (also see Appendix A) is given by,

$$\omega_{p,\vec{q}}^2 = \frac{q_c^2}{q^2} \omega_{p,c}^2 + \frac{q_{ab}^2}{q^2} \omega_{p,ab}^2 \quad (3)$$

The polar coupling requires that the phonon frequencies exceed the 3D screening frequency, which should be set by this $\omega_{p,\vec{q}}$. Hence, this implies that only phonons in a narrow cone around $q_{ab} \simeq 0$ can contribute to the polar couplings. It is questionable whether this small q_{ab} will show up in the polar couplings. Given the unknowns, this question is not easy to answer on theoretical grounds. On the other hand, leaving the overall strength aside, the frequency dependence of the electronic self-energy

can be easily calculated^{13,14} and in section III we will compare the experiment⁴ with the calculation, assuming the predominant electron-phonon coupling is due to the unscreened c-axis phonons.

II. REAL PART OF ELECTRON SELF-ENERGY

In the following, the real part of self-energy, $Re(\Sigma)$, contributed from interactions which can be captured by the c-axis optical dielectric function, $\epsilon_c(\omega)$, will be calculated where the strength of interactions as a function of energy is represented by the Eliashberg function, $\alpha^2 F(\omega)$. Regarding the empirical result shown in the experimental paper⁴, the main results in this paper are that a) the c-axis loss function, $Im(-1/\epsilon_c(\omega))$, is a good representative of $\alpha^2 F(\omega)$ for the optimally doped cuprate and b) when including screening effect, the expression of $\alpha^2 F(\omega)$ becomes Eq. (16) giving the good agreement of $Re(\Sigma)$ of the overdoped cuprate.

The electron self-energy can be given by ($\delta \rightarrow 0^+$),

$$\Sigma(\vec{p}, \epsilon) = -\frac{1}{(2\pi)^4 \pi} \int d^3 p_1 \int d\omega \int d\epsilon_1 Im W(\vec{p} - \vec{p}_1, \omega) \times \frac{Im G(\vec{p}_1, \epsilon_1)}{\omega + \epsilon_1 - \epsilon - i\delta} \left(\tanh \frac{\epsilon_1}{2k_B T} + \coth \frac{\omega}{2k_B T} \right) \quad (4)$$

where G and W are the retarded electron propagator and the effective interaction, respectively. Here we neglect the detailed momentum structure of the electron-phonon coupling, which although important for a subset of phonons (such as the B_{1g} and B_{1u} c-axis phonons), is motivated by the interest in small q phonons providing a more or less isotropic charge displacement along the c-axis. We neglect vertex corrections which may be important for polaron formation but are not crucial to develop the ideas of screening.

When only considering the interaction of electrons to polar c-axis phonons and electrons to electrons, the effective interaction (see Appendix B) can be written as

$$W_{eff}(\vec{q}, \omega) = \frac{v_q}{\epsilon_{tot}(\vec{q}, \omega)} \quad (5)$$

where $\epsilon_{tot}(\vec{q}, \omega) = \epsilon_{\infty} - v_q P_e(\vec{q}, \omega) + \epsilon_{ph}(\vec{q}, \omega)$ is the total dielectric function in which the core polarization, the phononic- and electronic polarizations, in terms of the electronic polarizability $P_e(\vec{q}, \omega)$, enter additively.

The effective interaction includes both Coulomb and EP interactions, and the manifestation of screening is that the interactions are mixed as Coulomb interactions modify the phonon propagator D and vice-versa. This effective interaction can be rewritten as¹³ (M_q is the bare EP vertex neglecting any fermionic momentum dependence)

$$W_{eff}(\vec{q}, \omega) = \frac{v_q}{\epsilon_{el}(q, \omega)} + \frac{\epsilon_{\infty}^2 M_q^2 D(q, \omega)}{\epsilon_{el}^2(q, \omega)} \quad (6)$$

where ϵ_{el} is the electronic polarizability Eq. (1) and $v_q = 4\pi e^2/q^2$; this is a general expression for phonon-modulated uniform charge displacements.

We now assert that the effective interaction W_{eff} is dominated by the coupling to the unscreened c-axis phonons. Next we assume that momentum dependences are smooth. This is definitely not problematic for the phonon-propagators hidden in W_{eff} because the important phonons are of the high energy optical variety having small dispersions. This is further helped by the fact that because of the metallic screening in the planar directions, only phonons with a small planar momentum q_{ab} can be regarded as unscreened. A more delicate issue relates to the electron momentum dependence of the bare vertex having implications for how the self-energy will depend on \vec{p} . Elsewhere we will show that this can give rise to highly interesting effects associated with the screening physics¹⁵ but here we will focus on the frequency dependences in a given momentum direction.

Neglecting momentum dependences, the phonon polarizability can be straightforwardly parameterized, by a sum over phonons with transversal frequencies ω_{Tj} , damping γ_j and strengths s_j , as tabulated by Tsvetkov *et al.*¹⁶,

$$\epsilon_{ph}(\omega) = \sum_j \frac{s_j \omega_{Tj}^2}{\omega_{Tj}^2 - \omega^2 + i\omega\gamma_j} \quad (7)$$

Taking for the electronic polarizability $v_q P_e(\omega) = \omega_{p,c}^2/\omega^2$ and a plasmon frequency $\omega_{p,c}$ large compared to all phonon frequencies one recovers the standard results for the EP coupling in metals, but we now focus on the category of unscreened phonons, such that $v_q P_e(\omega) = 0$.

In the insulator, the phonon propagator turns into the bare phonon propagator $D \rightarrow D^0$ which becomes in terms of the parametrization Eq. (7)

$$M_{q \simeq 0}^2 D^0(\omega) = -v_{q \simeq 0}^\infty \frac{\epsilon_{ph}(\omega)}{\epsilon_\infty + \epsilon_{ph}(\omega)}, \quad (8)$$

where $v_q^\infty = v_q/\epsilon_\infty$.

The Eliashberg function is defined as the Fermi-surface average¹³,

$$\alpha^2 F_{\vec{k}}(\omega) = \frac{1}{(2\pi)^3} \int \frac{d^2 k'}{v_F} \left| \frac{\epsilon_\infty M_{\vec{k}-\vec{k}'}}{\epsilon_{el}(\vec{k}-\vec{k}', \omega)} \right|^2 \text{Im} D(\vec{k}-\vec{k}', \omega) \quad (9)$$

while the real part of the electronic self-energy, calculated from the Eliashberg function, is given by¹⁴,

$$\text{Re} \Sigma(\vec{p}, \epsilon) = \int_0^\infty d\omega \alpha^2 F(\omega; \vec{p}, \epsilon) K\left(\frac{\epsilon}{kT}, \frac{\omega}{kT}\right) \quad (10)$$

where $K(y, y') = -\int_{-\infty}^\infty dx f(x-y) 2y'/(x^2 - y^2)$ with $f(x)$ being the Fermi distribution function.

A. $\alpha^2 F(\omega)$ for c-axis insulating system (optimally-doped)

Assuming smooth momentum dependences, and observing that in the insulator $\epsilon_{el} = \epsilon_\infty$, one immediately infers that the Eliashberg function for the polar phonons can be written as,

$$\alpha^2 F(\omega) = b \frac{|M_{q \simeq 0}^2|}{v_{q \simeq 0}} \text{Im} D^0(\omega) = b \cdot \text{Im} \left(-\frac{1}{\epsilon_{tot}(\omega)} \right) \quad (11)$$

where lumping together in the factor b is the numerical factors coming from the momentum integrations (see Appendix C). Since momentum dependences are weak we can as well take the optically measured c-axis loss function $\text{Im}(-1/\epsilon_c(\omega))$ where $\epsilon_c(\omega) = \epsilon_{tot}(q_{ab} = 0, q_c \rightarrow 0, \omega)$ as representative for the loss functions at small q_{ab} and arbitrary values of q_c . In this way, we obtained a good fit to the measured self-energy in the optimally doped cuprates⁴.

B. $\alpha^2 F(\omega)$ with metallic screening effect (overdoped)

In the following, we will include the metallic screening effect to calculate $\text{Re}(\Sigma)$ in the overdoped case. In the experimental paper⁴ we found that the self-energy in the overdoped system was reproduced in detail,

$$\alpha^2 F(\omega) = b \frac{\omega^2}{\omega_{src,c}^2 + \omega^2} \text{Im} \left(-\frac{1}{\epsilon_c(\omega)} \right) \quad (12)$$

using the loss function of the optimally doped system and a ‘filter’ function representing a characteristic ‘screening’ frequency $\omega_{src,c} \simeq 60\text{meV}$. As we will now argue, the ‘filter’ function $\omega^2/(\omega_{src,c}^2 + \omega^2)$ is consistent with the changes in the screening seen in optical spectroscopy. To incorporate the effect of the metallic screening, one could model the c-axis polarizability according to Eq. (1) as,

$$v_{q//c} P_e(q//c, \omega) = \frac{\omega_{p,c}^2}{\omega^2 + i\omega\Gamma} \quad (13)$$

We have neglected the details of the frequency and fermionic momentum dependence of the scattering rate. This simple Drude form is an over simplification but all what matters for the phonon screening are the overall energy scales of screening and the phonon frequencies. Moreover, we use “damping” as a way of loosely parameterizing the change from coherent metallic transport along the c -axis in overdoped systems to incoherent insulating behavior near optimal doping. The nature of this change is a very important issue, relating to charge confinement and/or the incoherent nature of anti-nodal quasi-particles governing c -axis propagation in an LDA treatment. A full description of this change is difficult around optimal doping where strong correlations are developed. An adequate description of the role of correlations requires treating both electronic correlations and

EP interactions on equal footing. Since such treatments are presently limited, we give only a heuristic picture of the consequences of strong damping and incoherence.

For finite $\omega_{p,c}$, $1/\epsilon_{el}$ will also acquire an imaginary part which contributes to the Eliashberg function. When the plasmon is underdamped while $\omega_{p,c}$ is in the phonon frequency window, the plasmon would become well ‘visible’ in the self-energy¹⁷. However, in the overdamped regime, $\Gamma \geq \omega_{p,c}$, of interest to the c-axis of the cuprates, this turns into a smooth background contribution. In the experimental determination of the self-energy such backgrounds are subtracted. Although it would be interesting to find out if such backgrounds associated with the c-axis metallization can be extracted from the experimental data, these should be ignored in the present context and we should focus on the phonon contribution to the effective interaction in Eq. (6),

$$W_{sc-ph}(\vec{q}, \omega) = \frac{M_q^2 D(\vec{q}, \omega)}{\epsilon^2(\vec{q}, \omega)} \quad (14)$$

where $\epsilon(\vec{q}, \omega) = \epsilon_{el}/\epsilon_\infty$ and ϵ_{el} is modeled according to Eq. (1). The renormalized phonon propagator¹³ is,

$$D(\vec{q}, \omega) = \frac{D^0(\vec{q}, \omega)}{1 - M_q^2 D^0(\vec{q}, \omega) P_e(\vec{q}, \omega)/\epsilon(\vec{q}, \omega)} \quad (15)$$

By using Eq. (9) and the same assumptions as for the optimally doped case, the Eliashberg function including the screening effect becomes,

$$\alpha^2 F(\omega) = b \frac{|M_{q \approx 0}^2|}{v_{q \approx 0}} \frac{1}{|\epsilon(\omega)|^2} \text{Im} D(\omega) \quad (16)$$

This more general form does reproduce the self-energies of both the overdoped and optimally-doped systems quite well, as long as the c-axis charge dynamics is not turning strongly underdamped.

Given the $\alpha^2 F(\omega)$ as in Eq. (16), the factor $|\frac{1}{\epsilon(\omega)}|^2$ acts like a filter function in the overdamped regime. The characteristic screening frequency $\omega_{scr,c}$ can be determined by demanding $|\frac{1}{\epsilon(\omega_{scr,c})}|^2 = 1/2$ such that the phonons with frequencies less than ω_{scr} can be regarded as screened. Since $\epsilon(\omega) = \epsilon_{el}(\omega)/\epsilon_\infty$ it follows immediately from Eq. (1),

$$\omega_{scr,c} = \frac{1}{\sqrt{2}} \left[\left((\Gamma^2 + 2\omega_{p,c}'^2)^2 + 4\omega_{p,c}'^4 \right)^{1/2} - (\Gamma^2 + 2\omega_{p,c}'^2) \right]^{1/2} \quad (17)$$

where $\omega_{p,c}' = \omega_{p,c}/\sqrt{\epsilon_\infty}$. In the overdamped regime ($\Gamma \gg \omega_{p,c}$), $\omega_{scr,c} \approx \frac{\omega_{p,c}}{\epsilon_\infty} \omega_{p,c}$ as in Eq. (2).

This $\omega_{scr,c}$ can be directly related to the electronic background in the optical conductivity, $\sigma_c^1(\omega)$. Eq. (1) leads to a simple Drude form for the conductivity which can be expanded in the regime $\Gamma \gg \omega$ as,

$$\sigma_1(\omega) = \frac{\omega_{p,c}^2}{4\pi\Gamma} \left(1 - \frac{\omega^2}{\Gamma^2} + \dots \right) \quad (18)$$

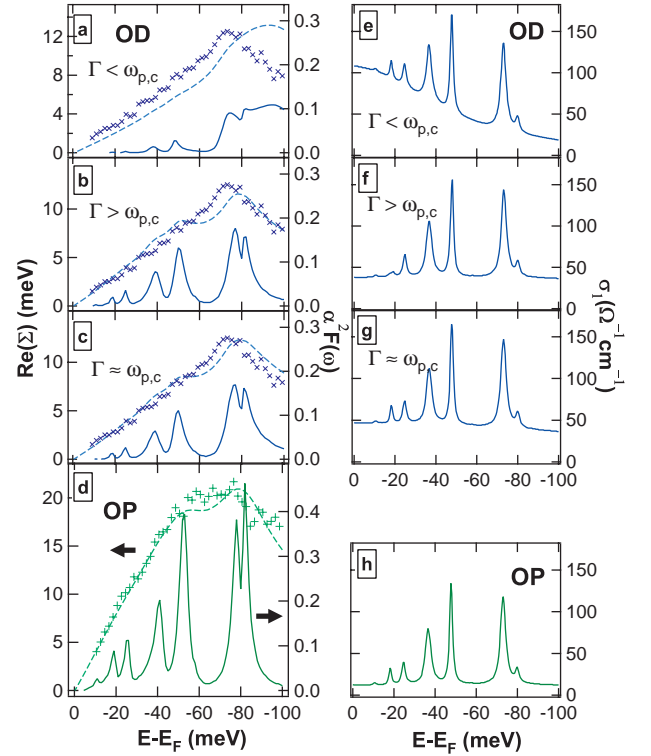


FIG. 1: The experimental c-axis optical conductivity in optimally doped (OP) from Ref. 16, (h). Various models for the optical conductivity of overdoped (OD) Bi2201 (e)-(g). The corresponding Eliashberg functions (solid line) and electronic self-energies (dash line) assuming that the predominant electron-phonon coupling is due to the unscreened c-axis phonons (a)-(d); experimental data in symbol are from Ref. 4. Parameters: (a)-(c), $\omega_{scr,c} \approx 60$ meV. (a) $\Gamma < \omega_{p,c}$, $\Gamma = 45$ meV and $\omega_{p,c} = 190$ meV, (b) $\Gamma > \omega_{p,c}$, $\Gamma = 430$ meV and $\omega_{p,c} = 350$ meV, and (c) $\Gamma \approx \omega_{p,c}$, $\Gamma = 180$ meV and $\omega_{p,c} = 250$ meV. (d) OP case, $\Gamma = 700$ meV and $\omega_{p,c} = 250$ meV.

and it follows from Eq. 2 that the height of this background corresponds to $\omega_{p,c}^2/4\pi\Gamma = (\epsilon_\infty/4\pi)\omega_{scr,c}$ in the overdamped regime ($\Gamma \gg \omega_{p,c}$). One notices that in principle the self-energy could be determined using the information in the optical conductivity, avoiding any free parameters. We note that since the optical data on overdoped Bi2201 are not available and we model these according to what has been measured in the $\text{La}_{2-x}\text{Sr}_x\text{CuO}_4$ (LSCO) system.

III. COMPARISON WITH EXPERIMENTAL DATA

According to Ref. 9, the ab plasma frequency $\omega_{p,ab} \approx 1$ eV while $\omega_{p,ab}/\omega_{p,c} \approx 4$ to 10 and we take $\omega_{p,c} \approx \omega_{p,ab}/4 \approx 250$ meV. To reconstruct the measured optical conductivity in the OP case¹⁶ [Fig. 1(h)] we need a large $\Gamma \sim 700$ meV to obtain a background $\approx 12 \Omega^{-1}\text{cm}^{-1}$. In Fig. 1(f)-(g) we combine the (dressed) phonon spectrum

of Bi2201 with the background as measured in the LSCO system at 30% doping¹¹, translating in an $\omega_{scr,c} \approx 60$ meV, indicating the insensitivity to the precise values of $\omega_{p,c}$ and Γ separately. In Fig. 1(b)-(d) we show the outcomes for both the Eliashberg functions and the calculated self-energies, finding results which closely track the phenomenological filter function used in Ref. 4.

For completeness we include the outcomes assuming a strongly underdamped plasmon [Fig. 1(a) and (e)]. One sees immediately that this yields a much less satisfactory outcome. We also notice that in the overdamped cases Fig. 1(b)-(d) the ‘phase space’ parameter $b \simeq 1$ in all cases while it has to be strongly reduced assuming the underdamped plasmon ($b \simeq 0.35$).

IV. CONCLUSION

We have demonstrated that the large scale changes found in the self-energy of the nodal quasiparticles in Bi2201 are in detailed quantitative agreement with the measured changes in the screening properties along the c-axis when it is assumed that this self-energy is mostly due to the scattering of the electrons against the polar phonons associated with the motions of ions in the c-direction. This is a direct evidence for the presence and importance of this type of interaction and in a future publication we will elaborate further consequences of this unconventional electron-phonon coupling¹⁵.

APPENDIX A: EFFECTIVE PLASMON FREQUENCY, $\omega_{p,\vec{q}}$

In a coupled layered electron gas, the dielectric function using the RPA approximation (Eq. (7) in Ref. 9) is given by

$$\epsilon(\omega, \vec{q}) = 1 - \frac{S}{\omega(\omega + i0^+)} \left\{ \frac{q_{ab}^2 \omega_{p,ab}^2}{q^2} p^0 \left(\frac{v_F q_{ab}}{\omega}, \frac{v_c q_c}{\omega} \right) + \frac{q_c^2}{q^2} \omega_{p,c}^2 p^0 \left(\frac{v_c q_c}{\omega}, \frac{v_F q_{ab}}{\omega} \right) \right\}$$

where S is a form factor, v_c is the effective velocity perpendicular to the layers, and p^0 is the function

$$p^0(a, b) \equiv \frac{2}{\pi a} \int_0^\pi \left\{ (1 - a \cos \phi)^2 - b^2 \right\}^{-1/2} \cos \phi d\phi$$

And, hence the effective 3D plasmon frequency $\omega_{p,\vec{q}}$ may be written as

$$\omega_{p,\vec{q}}^2 = \frac{q_{ab}^2}{q^2} \omega_{p,ab}^2 p^0 \left(\frac{v_F q_{ab}}{\omega}, \frac{v_c q_c}{\omega} \right) + \frac{q_c^2}{q^2} \omega_{p,c}^2 p^0 \left(\frac{v_c q_c}{\omega}, \frac{v_F q_{ab}}{\omega} \right)$$

where in the limit $\vec{q} \rightarrow 0$, $S \rightarrow 1$ and $p^0 \rightarrow 1$.

APPENDIX B: EFFECTIVE INTERACTION, W_{eff}

The detailed derivations of the following can be read from Ref. 13. When considering the single-process scattering of two electrons: i) by the unscreened electron-electron interaction and ii) by sending a phonon from one to the other, the combined interaction W^0 can be written as:

$$W^0(\vec{q}, \omega) = v_q^\infty + V_{ph}(\vec{q}, \omega)$$

where $v_q^\infty = 4\pi e^2/(q^2 \epsilon_\infty)$ is a bare Coulomb part and V_{ph} is a phonon mediated part.

This phonon mediated part (same as Eq. (8)) is given by,

$$V_{ph}(\vec{q}, \omega) = M_q^2 D^0(q, \omega)$$

where M_q is a bare EP vertex and D^0 is a bare phonon propagator.

Next, when considering all the possible of multiple-process scattering, the effective interaction in the classic RPA form, W_{eff} , can be written as:

$$W_{eff}(\vec{q}, \omega) = \frac{W^0(\vec{q}, \omega)}{1 - W^0(\vec{q}, \omega) P_e(\vec{q}, \omega)} = \frac{v_q}{\epsilon_{tot}(\vec{q}, \omega)}$$

where $\epsilon_{tot}(\vec{q}, \omega) = \epsilon_\infty - v_q P_e(\vec{q}, \omega) + \epsilon_{ph}(\vec{q}, \omega)$, $P_e(\vec{q}, \omega)$ is an electronic propagator and $\epsilon_{ph}(\vec{q}, \omega)$ is a phonon polarizability given by Eq. (7).

To explicitly separate the electron-electron part of the effective interaction, W_{eff} can be rewritten to be the same as Eq. (6) or:

$$W_{eff}(\vec{q}, \omega) = \frac{v_q}{\epsilon_{tot}(\vec{q}, \omega)} = \frac{v_q}{\epsilon_{el}(q, \omega)} + W_{sc-ph}$$

where W_{sc-ph} is the screened EP interaction given by Eq. (14) and the renormalized phonon propagator is given by Eq. (15).

APPENDIX C: NUMERICAL FACTOR, b

In the insulating case ($\epsilon_{el} = \epsilon_\infty$), from Eq. (9) and (11), b can be written as

$$b = \frac{\frac{1}{(2\pi)^3} \int \frac{d^2 k'}{v_F} |M_{\vec{k}-\vec{k}'}|^2 \text{Im} D^0(\vec{k} - \vec{k}', \omega)}{|M_{q \simeq 0}^2| \text{Im} D^0(\omega)}$$

In the overdoped case, replace M with $\epsilon_\infty M/\epsilon_{el}$ and D^0 with D in the above equation.

When momentum dependences are weak, the factor b can be approximated by

$$b \approx \frac{v_{q \simeq 0}}{(2\pi)^3} \int \frac{d^2 k'}{v_F}$$

ACKNOWLEDGMENTS

We thank D. van der Marel and A. Damascelli for enlightening discussions. SSRL is operated by the DOE Office of Basic Energy Science under Contract No. DE-AC02-76SF00515. ARPES measurements at Stan-

ford were supported by NSF DMR-0304981 and ONR N00014-04-1-0048. W.M. acknowledges DPST for financial support. T.P.D. would like to thank ONR N00014-05-1-0127, NSERC, and Alexander von Humboldt foundation. J.Z. acknowledges the support of the Fulbright foundation.

* non@stanford.edu

† On leave of absence from the Instituut-Lorentz for Theoretical Physics, Leiden University, Leiden, The Netherlands

¹ For the doping-dependent in-plane and out-of-plane resistivity of Bi2201 samples, respectively, Y. Ando, S. Komiya, K. Segawa, S. Ono, and Y. Kurita Phys. Rev. Lett. **93**, 267001 (2004); A. N. Lavrov, Y. Ando, and S. Ono, Europhys. Lett. **57**, 267 (2002).

² K. A. Muller and J. G. Bednorz, Science **237**, 1133 (1987)

³ C. Falter, G. A. Hoffmann, and F. Schnetgoke, J. Phys.: Condens. Matter **14**, 3239 (2002).

⁴ W. Meevasana, N. J. C. Ingle, D. H. Lu, J. R. Shi, F. Baumberger, K. M. Shen, W. S. Lee, T. Cuk, H. Eisaki, T. P. Devereaux, N. Nagaosa, J. Zaanen, and Z.-X. Shen, Phys. Rev. Lett. **96**, 157003 (2006).

⁵ For a recent review, see L. Pintschovius, Phys. Stat. Sol.(b) **242**, 30 (2005).

⁶ X. J. Zhou *et al.*, Phys. Rev. Lett. **95**, 117001 (2005); T. Cuk *et al.*, Phys. Stat. Sol. (b) **242**, 11 (2005). A. Lanzara *et al.*, Nature **412**, 510 (2001).

⁷ R. J. McQueeney, Y. Petrov, T. Egami, M. Yethiraj, G. Shirane, and Y. Endoh, Phys. Rev. Lett. **82**, 628 (1999).

⁸ S. Ishihara and N. Nagaosa, Phys. Rev. B **69**, 144520 (2004).

⁹ D. van der Marel and J.H Kim, J. Phys. Chem. Sol. **56**, 1825 (1995)

¹⁰ A.A. Tsvetkov, J. Schutzmann, J. I. Gorina, G. A. Kaljushnaia, and D. van der Marel, Phys. Rev. B **55**, 14152 (1996).

¹¹ S. Uchida, K. Tamasaku and S. Tajima, Phys. Rev. B **53**, 14558 (1996).

¹² H. Morawitz, I. Bozovic, V.Z. Kresin, G. Rietveld, and D. van der Marel, Z. Phys. B **90**, 277 (1993) and ref's therein.

¹³ G.D. Mahan, *Many Particle Physics* (Plenum Press, New York, 1981), ch.6, p. 560-566, 569-570 and 586-594.

¹⁴ G. Grimvall and E. Wohlfarth, *The Electron-Phonon Interaction in Metals*, (North-Holland, New York, 1981), ch.5, p. 98-107.

¹⁵ T.P. Devereaux *et al.*, to be published.

¹⁶ A.A. Tsvetkov, D. Dulic, D. van der Marel, A. Damascelli, G. A. Kaljushnaia, J. I. Gorina, N. N. Senturina, N. N. Kolesnikov, Z. F. Ren, J. H. Wang, A. A. Menovsky, and T. T. M. Palstra, Phys. Rev. B **60**, 13196 (1999).

¹⁷ M.E. Kim, A. Das and S.D. Senturia, Phys. Rev. B **18**, 6890 (1978); B.A. Sanborn, Phys. Rev. B **51**, 14256 (1995).